

Full-Scale Validation of Wind-Induced Response of Tall Buildings: Investigation of Amplitude-Dependent Dynamic Properties

Authors:

J. David Pirnia, University of Notre Dame, Notre Dame, IN, jpirnia@nd.edu
Tracy Kijewski-Correa, University of Notre Dame, Notre Dame, IN, tkijewsk@nd.edu
Ahmad Abdelrazaq, Samsung Engineering & Construction Group, Seoul, Korea, ahmad.abdelrazaq1@samsung.com
Jaeyong Chung, Samsung Research Institute, Seoul, Korea, jae.chung@samsung.com
Ahsan Kareem, University of Notre Dame, Notre Dame, IN, kareem@nd.edu

ABSTRACT

This study investigates the effect of amplitude-dependence on the dynamic properties of a 865 ft (264 m) tall residential building. The amplitude-dependent features of this building are investigated using a time domain approach and are compared to existing models in the literature. In particular, this study highlights the impact of amplitude-dependent frequency on damping estimates by traditional spectral methods.

INTRODUCTION

Dynamic properties such as frequency and damping must be accurately estimated early in the design process to allow for wind tunnel prediction of equivalent static wind loads and accelerations necessary for tall building design. While frequencies can be reasonably estimated, damping proves to be far more difficult to quantify due to its reliance on a number of structural and nonstructural features. Most of the predictive damping models are drawn from databases characterized by a significant amount of scatter [Satake et al., 2003]. This scatter is not only due to the uncertainty in estimating damping itself, but also from the fact that damping and even frequency often possess a measurable level of amplitude-dependence that results from imposing a linear model on an inherently nonlinear structure. In general, published estimates of dynamic properties rarely take this into account. However, as demonstrated by Li et al. [2003], this amplitude-dependence can result in larger acceleration responses, particularly in the acrosswind direction. While some models for amplitude-dependence have been proposed in the literature [e.g., Jeary, 1986], their appropriateness for tall, flexible structures has not been verified. It is precisely this class of structure, however, that is governed by habitability limit states most affected by damping levels. This has motivated recent efforts by Li et al. [2003; 2005; 2006] to document in-situ amplitude dependence in tall buildings such as the DiWang Building, Central Plaza, Jin Mao, and Bank of China. Fortunately, through continued full-scale monitoring of tall, flexible structures by a number of authors, and through advancements in system identification methods, the quality of existing damping databases can be refined and expanded, while the effect of amplitude-dependence can be documented to produce more reliable estimates of in-situ damping levels for tall, flexible buildings.

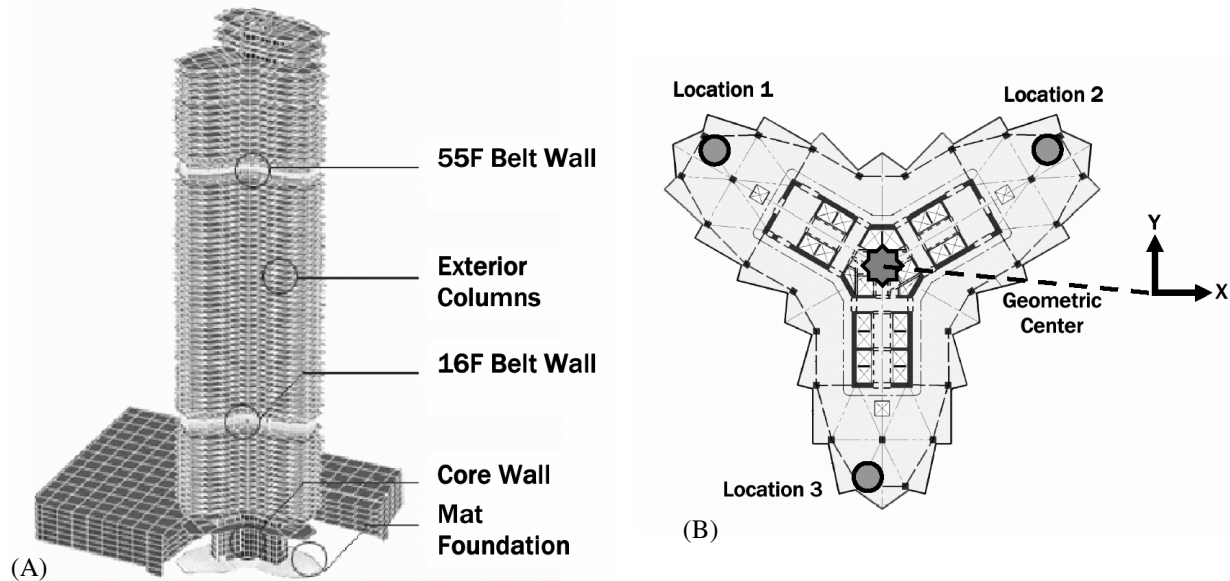


FIGURE 1 - BUILDING DIAGRAMS: (A) ELEVATION VIEW WITH STRUCTURAL FEATURES; AND (B) 64TH FLOOR PLAN SHOWING INSTRUMENTATION LOCATIONS AND GLOBAL SWAY AXES

This study furthers this effort by documenting the amplitude-dependence of frequency and damping in a composite high rise, with comparisons to existing models in the literature. Various regimes of damping are discussed in this study, and the role of amplitude-dependence in frequency is explored as an underlying source of inflated spectral damping estimates.

BUILDING DESCRIPTION & INSTRUMENTATION OVERVIEW

The building considered here is a 73-story, 865 ft (264 m) tall composite residential high-rise located in Seoul, South Korea. Lateral loads are resisted through an indirect outrigger belt wall system at the mechanical levels (16 to 17, and 55 to 56) that link the exterior columns to the reinforced concrete core, as shown in Figure 1A. Additional information on the design and construction of this building can be found in Abdelrazaq, et al. [2005]. Most relevant to this discussion is the building mode shapes and periods of vibration predicted from finite element modeling (FEM), as summarized in Figure 2. Note that all three modes do manifest some degree of coupling.

The building is equipped with three orthogonal pairs of Wilcoxon 731A/P31 seismic accelerometers mounted to girders at three locations on the 64th floor (64F), as shown in Figure 1B. Filtered outputs from the six accelerometers are projected onto the X - and Y -axes of the building in order to capture the sway response along those two axes, in addition to the torsional response. As such, the discussions which follow will reference X - and Y -sway and torsional responses at each of these three locations. The building response data is supplemented by an FT Technologies FT702 ultrasonic anemometer mounted atop a 2 m mast at the north end of the building's rooftop.

Output from the accelerometers and anemometer are received by a 12-bit IOtech Wavebook/512A data acquisition unit. Based on the accelerometer's sensitivity, the system's configuration achieves an approximate resolution of 0.001 milli-g. Data is sampled at 10 Hz and

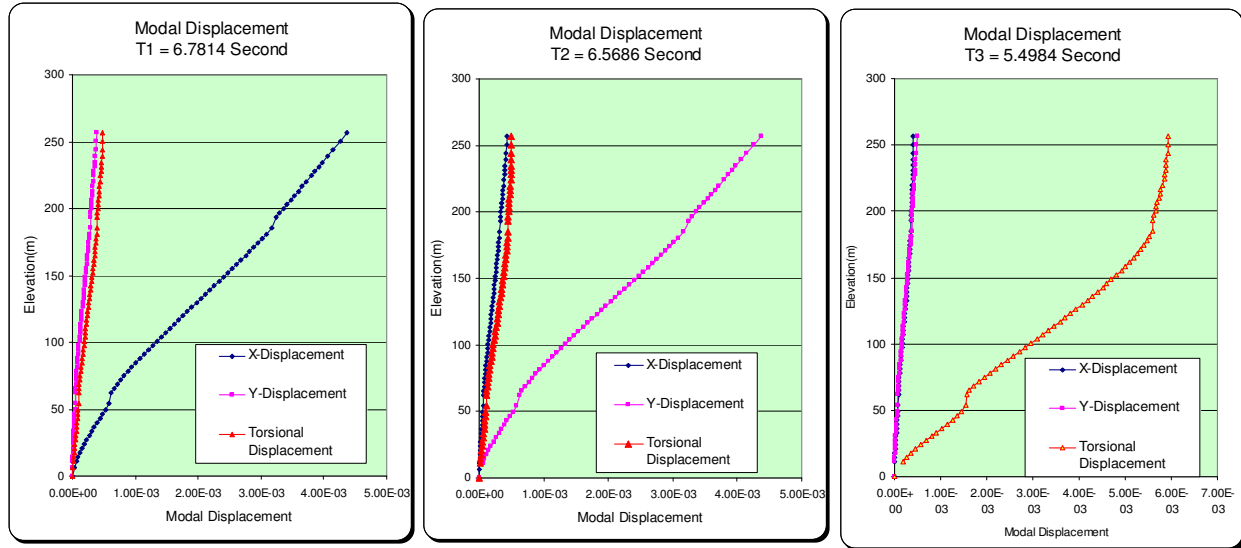


FIGURE 2 - FEM PREDICTED MODE SHAPES AND PERIODS [ABDELRAZAQ ET AL., 2005]

archived on an on-site computer via DASYlab software. Off-site access is permitted via an FTP server.

SPECTRAL APPROACH TO EXTRACT DYNAMIC PROPERTIES

Over 800 hours of ambient response data collected during November and December, 2006 is now considered. It is important to note that the estimated dynamic properties are drawn from a limited data set under relatively low-amplitude responses. The database was analyzed by a Fourier spectral approach to determine the dynamic properties in-situ. In order to minimize spectral bias errors to approximately -5%, the data was divided into blocks of 8192 points and fast Fourier transformed and averaged to produce the power spectral density (PSD) [Bendat and Piersol, 2000]. The resulting PSDs were derived from 3806 transformed blocks of data, resulting in a spectral variance of approximately 0.03%. The frequency and critical damping ratios associated with each spectral peak were extracted via the Half Power Bandwidth Method (HPBW) [Bendat and Piersol, 2000].

Table 1 summarizes the dynamic properties estimated from each response component, reporting the mean value accompanied by the coefficient of variation (CoV) determined by averaging the properties extracted from each sensor. As expected, frequency values were identified with a greater certainty (lower CoV) than the critical damping ratios. Still, reasonably good repeatability is noted for the damping values at each location (CoV < 10%). These values are also consistent with those extracted from earlier data recorded prior to 2006 [Abdelrazaq et al., 2005].

Table 1 also compares the designer predictions/assumed values to the dynamic properties extracted in this spectral approach. Design periods of vibration were obtained from an FEM of the building, while the design critical damping ratios were based on levels commonly assumed for this type of construction [Abdelrazaq et al., 2005]. The table also summarizes the relative participation of each mode in the overall response, which was captured well by the FEM. Note that for all three response components, periods of vibration were all almost 25% lower than the designer's predictions. This consistency indicates that the modeling of the overall system

Mode Characteristics	Mode 1 <i>Dominant x-sway, slight y-sway and torsion</i>		Mode 2 <i>Dominant y-sway, slight x-sway and torsion</i>		Mode 3 <i>Dominant torsion, slight x- and y- sway</i>	
	Frequency [Hz]	Damping [%]	Frequency [Hz]	Damping [%]	Frequency [Hz]	Damping [%]
FEM (Participation)	0.147 (1.0)	1.5	0.152 (0.97)	1.5	0.182 (0.81)	1.5
In-Situ <CoV> (Participation)	0.197 <0.0%> (1.0)	1.7 <3.4%>	0.206 <0.0%> (0.96)	1.3 <2.8%>	0.241 <0.0%> (0.82)	1.6 <3.3%>

TABLE 1 - COMPARISON OF FEM AND IN-SITU PERIODS AND CRITICAL DAMPING RATIOS

behavior was accurate, though some general properties of the structural materials (e.g., Young's Modulus) may differ in-situ. In serviceability design, composite structures are generally assumed to have a critical damping ratio around 1.5%; therefore the observed critical damping ratios are quite consistent with these design assumptions.

RANDOM DECREMENT APPROACH TO EXTRACT DYNAMIC PROPERTIES

The Random Decrement Technique (RDT) is an effective tool to obtain decay curves for system identification and has some additional advantages in cases where non-stationarity and even modest non-linearity of the system are suspected. Although linearity of the system is a basic assumption of the classic interpretation of RDT [Vandiver et al., 1982], Tamura and Sugauma [1996] found that amplitude-dependent results referenced to a peak trigger (zero slope and arbitrary amplitude) could be determined provided that the damping and frequency estimates are extracted from the initiation of the Random Decrement Signature (RDS). This approach is adopted herein. Once the RDS is obtained by this strict trigger condition, it is Hilbert transformed and the frequency and damping are respectively extracted by best-fits to cycles 0.5-3.5 of the phase and amplitude of the resulting analytic signal. To reduce some of the sensitivity associated with the trigger condition, a local averaging scheme was employed [Kijewski-Correa et al., 2006], where five equally spaced triggers within a range of +/-3% of the actual trigger were utilized in the RDT, and the dynamic properties from the resulting RDSs were averaged. The focus herein will be on the lateral responses of the building, which were isolated in the time histories using bandpass filters before applying the RDT.

An analysis was performed to extract information about the amplitude-dependence of the building's dynamic properties. The analysis utilized 50 triggers equally spaced within the interval of 0.2 to 1 milli-g, retaining only results generated from a minimum of 200 averages. Finally, each response component was analyzed separately to account for variations in the accelerations recorded at each of the three locations.

Over 800 hours of data were used to obtain the amplitude-dependent curve for both the fundamental *X-sway* response, provided in Figure 3 and summarized in Table 2A, and the fundamental *Y-sway* response, provided in Figure 4 and summarized in Table 2B. The following discussion expands upon these results.

Response	Frequency [Hz]				Critical Damping Ratio [%]			
	Amp 1 ¹	Amp 2 ²	Amp 3 ³	Amp 4 ⁴	Amp 1 ¹	Amp 2 ²	Amp 3 ³	Amp 4 ⁴
Location 1 X	0.1987	0.1986	0.1982	0.1975	1.82	1.06	0.86	0.86
Location 2 X	0.1992	0.1988	0.1982	0.1975	0.65	0.54	0.64	0.76
Location 3 X	0.1984	0.1984	0.1985	0.1979	2.03	1.88	1.01	0.86
Average <CoV>	0.1987 <0.2%>	0.1986 <0.1%>	0.1983 <0.1%>	0.1976 <0.1%>	1.50 <49.5%>	1.16 <58.2%>	0.84 <22.0%>	0.83 <6.9%>

Result of trigger level = ¹ 0.10 milli-g; ² 0.20 milli-g; ³ 0.40 milli-g; ⁴ 0.60 milli-g

(A)

Response	Frequency [Hz]				Critical Damping Ratio [%]			
	Amp 1 ¹	Amp 2 ²	Amp 3 ³	Amp 4 ⁴	Amp 1 ¹	Amp 2 ²	Amp 3 ³	Amp 4 ⁴
Location 1 Y	0.2073	0.2070	0.2066	0.2062	0.55	0.47	0.50	0.48
Location 2 Y	0.2071	0.2068	0.2064	0.2059	0.50	0.53	0.58	0.58
Location 3 Y	0.2071	0.2071	0.2066	0.2060	1.07	0.58	0.43	0.39
Average <CoV>	0.2072 <0.1%>	0.2070 <0.1%>	0.2065 <0.1%>	0.2060 <0.1%>	0.71 <44.9%>	0.53 <10.9%>	0.50 <14.8%>	0.48 <19.1%>

Result of trigger level = ¹ 0.10 milli-g; ² 0.20 milli-g; ³ 0.40 milli-g; ⁴ 0.60 milli-g

(B)

TABLE 2 - SELECTED AMPLITUDE-DEPENDENT RESULTS FOR (A) X- AND (B) Y-SWAY RESPONSE

FREQUENCY DISCUSSION

It is widely understood that stiffness (frequency) reduces with amplitude of motion, which is affirmed for both lateral responses, even over the limited amplitude range considered here. As expected, there is consistency between the outputs of all three sensors in each direction (Figures 3 and 4) and with the HPBW results in Table 1. A linear fit to the outputs at Location 1 indicates a softening of frequency in the *X-sway* from its low amplitude by a factor of 0.0027 \ddot{x} . For the *Y-sway*, the frequency softens by a factor of 0.0023 \ddot{x} . Thus the degree of amplitude dependence is more pronounced in the *X-axis*. While the variation in frequency is less than a percent over the amplitude range considered, it will be demonstrated later that this can have significant influences on damping estimation.

DAMPING DISCUSSION

Interestingly, the damping results demonstrate two distinct regimes. For the *X-sway*, damping values observed at the various locations converge when the peak responses exceed 0.4 milli-g. The inset PSDs in Figure 3 help explain the source of this behavior. In the low amplitude regime, the resonant response is quite modest compared to the noise floor. Even though each result generally contains more than 1000 averaged segments in this regime, the influence of these contributions still infiltrates the RDT algorithm, and the resonant contribution cannot be fully isolated, leading to inaccurate damping estimates. As the resonant amplitude increases, its participation in the overall response becomes more significant, and it can be isolated. This results in the converged damping value of 0.84% (Table 2A). Note that this value is approximately half the damping value observed previously in the HPBW analysis (Table 1). Similarly for the *Y-*

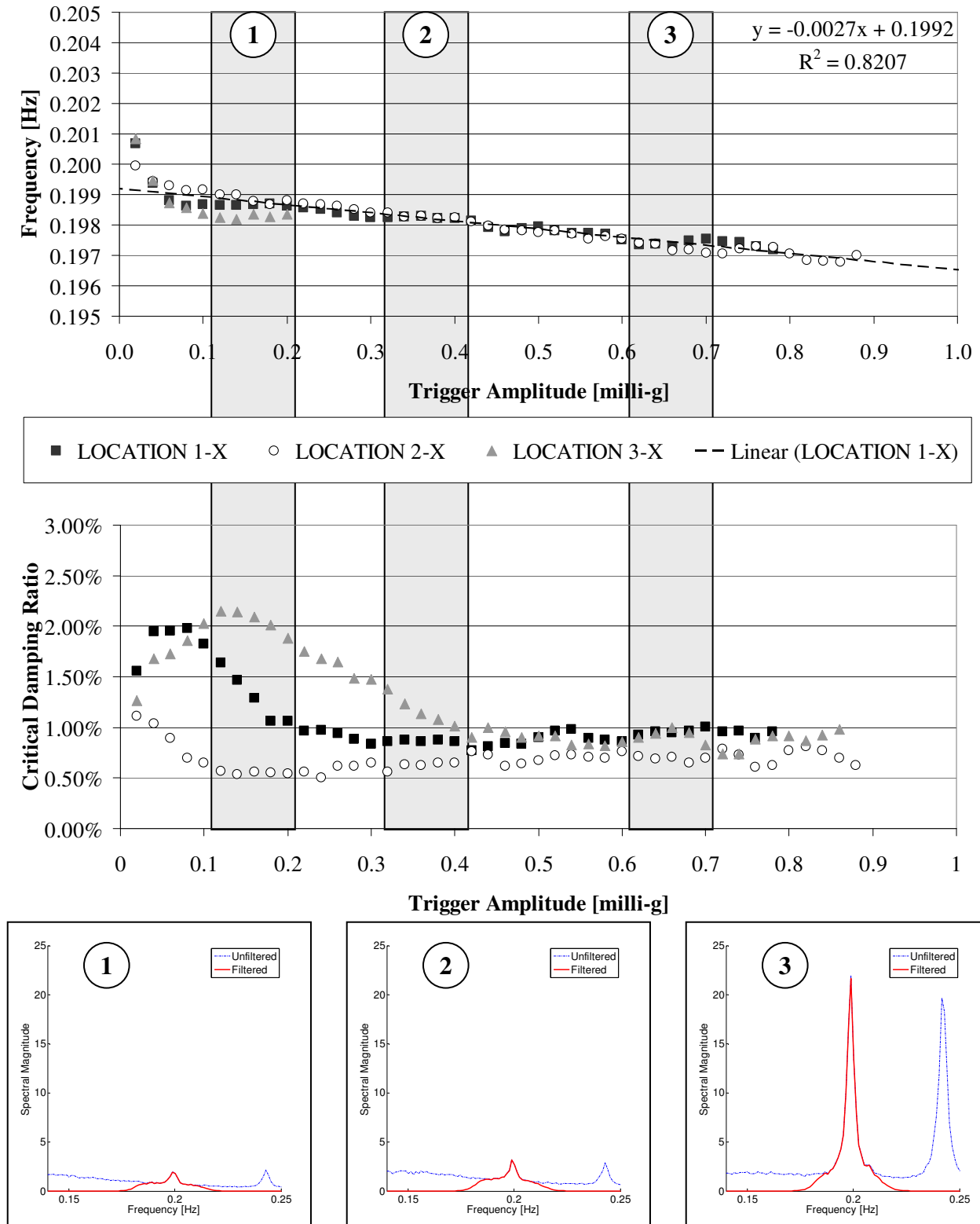


FIGURE 3 - AMPLITUDE-DEPENDENT FREQUENCY AND CRITICAL DAMPING RATIO, X-SWAY, WITH INSET PSDS FOR THREE AMPLITUDE REGIMES

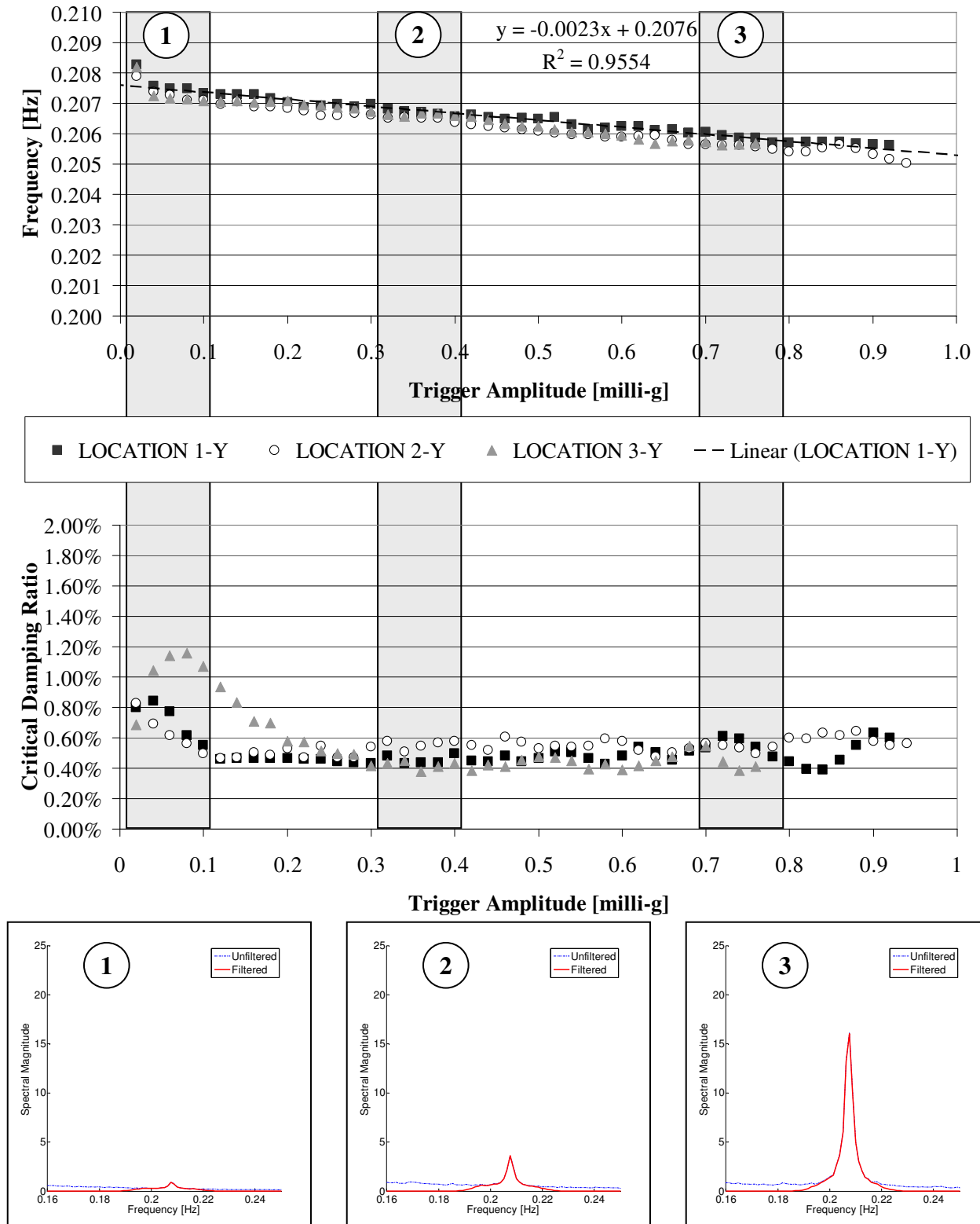


FIGURE 4 - AMPLITUDE-DEPENDENT FREQUENCY AND CRITICAL DAMPING RATIO, Y-SWAY; WITH INSET PSDS FOR THREE AMPLITUDE REGIMES

sway, damping values observed at the various locations converge when the peak responses exceed 0.2 milli-g, despite the *X*- and *Y*-sway responses having overall comparable response levels. It becomes apparent from the inset PSDs in Figure 4 that a slight coupling with the *X*-sway response at low amplitude levels infiltrates the RDT analysis and again leads to inflated damping values. Beyond 0.2 milli-g, a stabilized damping value of approximately 0.5% is observed (Table 2B), again less than half of the previous HPBW result (Table 1). However, the stabilized damping values for this building are consistent with the values noted in RDT analyses conducted on other composite and reinforced concrete tall buildings: Di Wang Building ($\xi \sim 0.6\%$) [Li et al., 2005], Central Plaza ($\xi \sim 0.5\%$) [Li et al., 2005], Jin Mao ($\xi \sim 0.55\%$), [Li et al., 2006], and Bank of China ($\xi \sim 0.4\%$) [Li et al., 2003]; and underscore that damping is oftentimes less than assumed serviceability standards at low amplitudes.

It should be noted that damping values reported in this study do not show the characteristic increase with amplitude proposed by Jeary [1986] and subsequently documented in-situ by Li et al. [2003; 2005]. This may be due to the fact that responses observed here are relatively small, possibly resigning this data to the low-amplitude plateau of the classic amplitude-dependent model.

While the larger damping values in the low amplitude regimes can be justified by considering the infiltration of adjacent spectral energy into the RDT process, the discrepancies between stabilized RDT values and HPBW results is troubling. Although it is understood that spectral bias will lead to overestimates of damping, considering the resolution used in the spectral analysis, these biases are not sufficient to explain these differences. Instead, it is likely traced to the amplitude-dependence of the natural frequencies. A simple demonstration of this concept begins with the HPBW definition (1).

$$\beta = 2\xi f_n \quad (1)$$

As discussed in Kijewski-Correa and Kareem [2006], harmonic-type analyses will produce spectral representations that peak at the mean frequency representative of the average frequency of oscillation, while any variation in the frequency of oscillation will be carried in the system's bandwidth, thus affecting the damping value. Next assume damping can be treated as a constant, which seems to be supported by the stabilized representations in Figures 3 and 4. If a system's frequency varies between two limiting values (f_1 , f_2), then the effective HPBW about each of these limiting frequencies will be: $\beta_A = 2\xi f_1$ and $\beta_B = 2\xi f_2$, respectively, as shown in Figure 5. Since the Fourier Transform has no ability to detect frequency variations, it will treat this phenomenon by a widened spectral peak encompassing both limiting frequency values and their respective bandwidths, centered at net (mean) frequency: $f_{net} = (f_1 + f_2)/2$. Thus the total bandwidth of this combined system is given by (2).

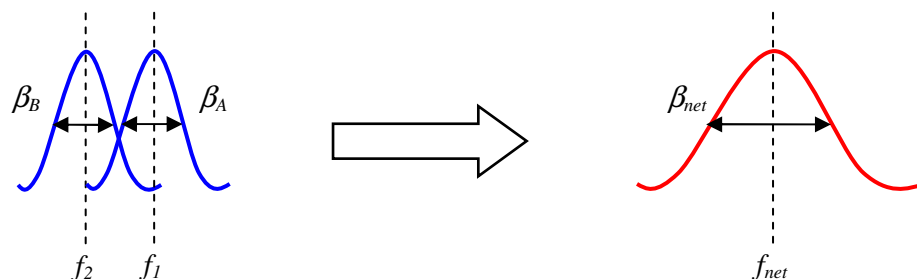


FIGURE 5 - SCHEMATIC OF FOURIER REPRESENTATION OF SYSTEM WITH VARYING FREQUENCIES

$$\beta_{net} = (f_1 + \beta_A / 2) - (f_2 - \beta_B / 2) = f_1 + \xi f_1 - f_2 + \xi f_2 = (f_1 - f_2) + \xi(f_1 + f_2) \quad (2)$$

The unsuspecting analyst, applying (1) to this system, will find a net damping value given by (3).

$$\xi_{net} = \frac{(f_1 - f_2) + \xi(f_1 + f_2)}{(f_1 + f_2)} \quad (3)$$

Applying (3) to the data at hand (Table 3), demonstrates that the use of a HPBW analysis on a system with even a slightly amplitude-dependent frequency results in damping values that can be 30-60% larger than the actual damping associated with the system. Again a Fourier analysis is ill-equipped to handle frequency variations, and thus underscores the importance of time-domain approaches for system identification. This demonstration may explain the discrepancies noted between HPBW and RDT damping values, and potentially those noted by other authors.

	Frequency [Hz]			Critical Damping Ratio		
	f ₂	f ₁	Difference	ξ	ξ _{net}	Difference
X-sway	0.1976	0.1987	-0.56%	0.84%	1.12%	-33%
Y-sway	0.2060	0.2072	-0.58%	0.50%	0.79%	-58%

TABLE 3 - IMPACTS OF AMPLITUDE-DEPENDENT DAMPING ON SPECTRAL DAMPING ESTIMATES

CONCLUSIONS

This study investigated the effect of amplitude-dependence on the dynamic properties of a 865 ft (264 m) tall composite residential building. Initial spectral analyses in this and a previous study documented damping values consistent with design assumptions and periods of vibration 25% less in-situ. However, an amplitude-dependent analysis using the Random Decrement Technique demonstrated the amplitude-dependence in frequency and a markedly lower stabilized damping value, akin to that observed for other tall, flexible buildings. A simplified example demonstrated that despite a relatively constant damping value, subtle frequency variations will affect the bandwidth of any Fourier spectrum, resulting in larger HPBW damping estimates. This underscores the need for analysis frameworks capable of accommodating amplitude-dependence in tall, flexible structures.

ACKNOWLEDGEMENTS

The authors wish to acknowledge the financial support and cooperation of Samsung Corporation and NSF Grant CMS 06-01143. The authors also wish to acknowledge their wider collaboration with Skidmore Owings and Merrill and the Boundary Layer Wind Tunnel Laboratory at the University of Western Ontario on this project.

REFERENCES

- [1] Abdelrazaq, A., Kijewski-Correa, T., Young-Hoon, S., Case, P., Isyumov, N., et al., "Design and Full-Scale Monitoring of the Tallest Building in Korea: Tower Palace III", *Proceedings of 6th Asia-Pacific Conference on Wind Engineering*, Seoul, Korea, September 2005.
- [2] Bendat, J. and A. Piersol, *Random Data: Analysis and Measurement Procedures*, John Wiley & Sons, New York, NY, 2000.

- [3] Jeary, A.P., "Damping in tall building—A mechanism and predictor", *Earthquake Engineering and Structural Dynamics*, Vol. 14, 1986, pp. 733-750.
- [4] Kijewski-Correa, T. and Kareem, A., "Efficacy of Hilbert and wavelet transforms for time-frequency analysis," *Journal of Engineering Mechanics, ASCE*, Vol. 132(10), 2006, pp.1037-1049.
- [5] Kijewski-Correa, T., Kilpatrick, J., Kareem, A., Kwon, D.K., Bashor, R., et al., "Validating Wind-Induced Response of Tall Buildings: Synopsis of the Chicago Full-Scale Monitoring Program", *Journal of Structural Engineering*, Vol. 132, 2006, pp. 1509-1523.
- [6] Li, Q.S., Yang, Ke., Wong, C.K., and A.P. Jeary, "The effect of amplitude-dependent damping on wind-induced vibrations of a super tall building", *Journal of Wind Engineering and Industrial Aerodynamics*, Vol. 91, 2003, pp. 1175-1198.
- [7] Li, Q.S., Xiao, Y.Q., and C.K. Wong, "Full-scale monitoring of typhoon effects on super tall buildings", *Journal of Fluids and Structures*, Vol. 20, 2005, pp. 697-717
- [8] Li, Q.S., Fu, J.Y., Xiao, Y.Q., Li, Z.N., Ni, Z.H., et al., "Wind tunnel and full-scale study of wind effects on China's tallest building", *Engineering Structures*, Vol. 28, 2006, pp. 1745-1758.
- [9] Satake, N., Suda, K., Arakawa, T. Sasaki, A., and Y. Tamura, "Damping evaluation Using Full-Scale Data of Buildings in Japan", *Journal of Structural Engineering*, Vol. 129(4), 2003, pp. 470-477.
- [10] Tamura, Y., and S. Suganuma, "Evaluation of amplitude-dependent damping and natural frequency of buildings during strong winds", *Journal of Wind Engineering and Industrial Aerodynamics*, Vol. 59, 1996, pp. 115-130.
- [11] Vandiver, J., Dunwoody, A., Campbell, R., and M. Cook, "A Mathematical Basis for Random Decrement Vibration Signature Analysis Technique", *Journal of Mechanical Design*, Vol. 104, 1982, pp. 307-313.